

## Original

# The Effects of Implant Surface Characteristics on Surrounding Bone: A Comparative Study of Two Types of Surface Characteristics

Kazuko Yamamoto<sup>1)</sup>, Tsukasa Yanagi<sup>1)</sup>, Akira Watazu<sup>2)</sup>, Kay Teraoka<sup>2)</sup> and Hirofumi Kido<sup>1)</sup>

<sup>1)</sup> Section of Oral Implantology, Department of Oral Rehabilitation, Fukuoka Dental College, Fukuoka, Japan

<sup>2)</sup> National Institute of Advanced Industrial Science and Technology (AIST), Nagoya, Japan

(Accepted for publication, December 10, 2013)

**Abstract:** The aims of this study were to create experimental implants by coating rough plastic surfaces with a thin layer of titanium, and to use the experimental implants in an animal experiment to investigate whether differences in the surface characteristics of the implant affect the peri-implant bone reaction during the period of osseointegration. Titanium rods of diameter 1.6 mm and length 7 mm were treated by acid etching (AE) or sandblasting followed by acid etching (SA), and replicas were made from plastic. Experimental implants were created by depositing a thin layer of titanium on the plastic replicas by DC-magnetron sputtering, and the surface characteristics of the experimental implants were evaluated. The experimental implants were placed in the tibias of eight-week-old male SD rats. The rats were sacrificed and the implants harvested at 3, 5, 10, 14, 21 and 28 days after implant placement. The samples were examined by optical microscopy and micro-CT to confirm peri-implant new bone growth. Examination of the experimental implants by SEM imaging showed that the different surface conditions (SA and AE) had been faithfully recreated. TEM observation and XPS analysis confirmed that the coating was titanium. The surface roughness of SA and AE was  $2.68 \pm 0.536 \mu\text{m}$  and  $0.47 \pm 0.069 \mu\text{m}$ , respectively. With AE, the BMD of peri-implant trabecular bone showed that bone mineralization progressed not on the surface of the implant but at sites a small distance away. At day 28 after placement of the implant, when osseointegration was complete, the BMD value in the region near the implant surface was higher in SA than in AE. Furthermore, the BV/TV value was high at an earlier stage in SA than AE. The results showed that the SA surface was better than the AE surface for achieving osseointegration.

**Key words:** Implant, Surface characteristics, Titanium coating, Micro-CT, Animal study

## Introduction

Osseointegration is the criterion on which the success of an oral implant is assessed in current practice. Research has been carried out over a considerable time into modifications of the implant surface with the aim of achieving sound osseointegration at the earliest possible stage following implant placement. The results have shown that osseointegration is established relatively early with implants processed to give a surface roughness in the order of  $2 \mu\text{m}$ , and the clinical data have been favorable<sup>1-5)</sup>. However, there has been little detailed investigation of the effects of the characteristics of the surface roughness of the implant on the reaction of the peri-implant bone, and it is not clearly known whether there is any variation in the reaction of the surrounding bone due to differences in the characteristics of the rough surface.

In the present study, experimental implants were created by coating plastic implants that had two different types of surface characteristics with a thin layer of titanium in order to examine

the bone reaction near the implant surface. One surface texture replicated etching with acid (AE), the other replicated sandblasting followed by acid etching (SA).

The aims of this study were to create experimental implants by coating rough plastic surfaces with a thin layer of titanium, and to use the experimental implants in an animal experiment to investigate whether differences in the surface characteristics of the implant affect the peri-implant bone reaction during the period of osseointegration.

## Materials and Methods

### Creation of experimental implants

In this experiment, implants with two different types of surface characteristics were created. First, the surfaces of titanium rods of 1.6 mm diameter  $\times$  7 mm length were treated by either acid etching (AE) or sandblasting followed by acid etching (SA). Impressions of each rod were taken using impression material (Imprint™, 3M ESPE, Saint Paul, USA), and epoxy resin (Epon 812, Taab, Aldermaston, UK) was poured into the negative impression cast. The resin was degassed under negative pressure

Correspondence to: Dr. Hirofumi Kido, Section of Oral Implantology, Department of Oral Rehabilitation, Fukuoka Dental College, 2-15-1 Tamura, Sawara-ku, Fukuoka, 814-0193 Japan; Tel: +81-92-801-0411; Fax: +81-92-801-0513; E-mail: hkido@college.fdcnet.ac.jp

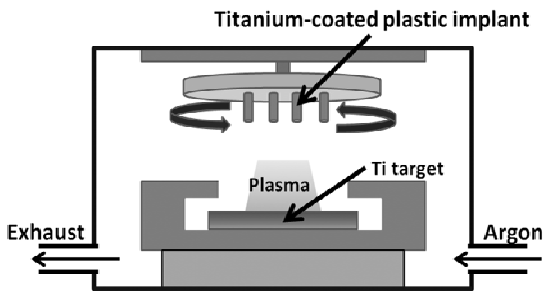


Figure 1. The schema of the DC magnetron sputtering apparatus.

for approximately 1 h, heated at 35 °C for 24 h, and then polymerized at 45 °C for 24 h and 60 °C for 48 h to produce rough-surfaced plastic rods. The plastic rods with each of the two types of surface texture were then coated with a thin layer of titanium, according to the method of Watazu et al.<sup>6-8)</sup> A DC-magnetron sputtering device (Astellatech, Inc., Kanagawa, Japan) was used with a titanium target of 99.9% purity, and sputtering was carried out for 43 min using 200 W DC power under a 0.5 Pa argon atmosphere (Fig. 1) (Table 1). The experimental implants (1.6 mm diameter × 7 mm length) were evaluated.

**Evaluation of experimental implants**

**Evaluation by scanning electron microscopy**

The titanium rod and its replica, the titanium-coated plastic implant, were imaged using a scanning electron microscope (SEM) (JSM-6330F, S3500N, JEOL Ltd., Tokyo, Japan). The shape of the surface was compared between images. The Sa (the arithmetic average of the 3D height of the roughness) and the Sdr (the developed surface area ratio) of SA and AE experimental implants were compared.

**Evaluation of surface roughness**

A 3D laser scanning microscope (VK-X100; KEYENCE Co., Osaka, Japan) was used to measure the shape of the surface.

**Evaluation by transmission electron microscopy**

The experimental implant was embedded in EPON812 (TAAB, Aldermaston, UK), and the specimens were sectioned (slice thickness: 70 nm) by using microtome (REICHERTNISSEI-ULTRACUT S, Leica, Wetzlar, Germany) with a diamond-knife (DiATOME ultra 45 °; NISSHIN EM Co., Ltd., Tokyo, Japan). Ultrathin sections were prepared for examination of the titanium coating in cross section by a transmission electron microscope (TEM) (1200-EX; JEOL Ltd., Tokyo, Japan) in order to evaluate the formation state of the titanium coating.

**Evaluation of surface characteristics**

The surface composition of the two types of experimental implant was detected using X-ray spectroscopic analysis (XPS)

Table 1. DC sputtering apparatus condition for titanium coating.

- Target: 99.9% Titanium
- DC power: 200 W
- Sputtering gas: Ar
- Ar pressure: 0.5 Pa
- Deposition time: 43min
- Deposition temperature: Room temperature
- Distance between the Ti target and plastic implant: 100mm

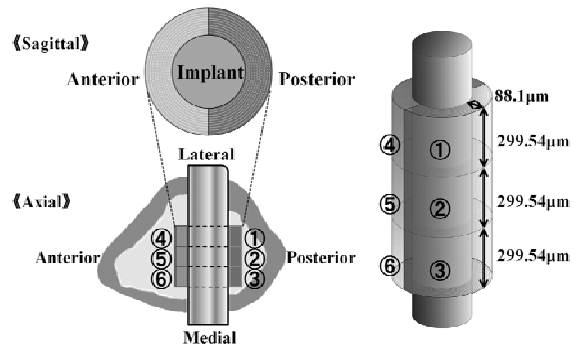


Figure 2. Evaluation by micro-CT. Bone volume and bone mineral density were measured 0-88.1 μm from the surface of the implant.

(Quantum 2000, ULVAC-PHI, Inc., Kanagawa, Japan). The instrument is equipped with a monochromatic x-ray source (Al K $\alpha$  anode) operating at 15 kV and 30 W. The diameter of the analyzed spot was approximately 200 μm, the angle between the electron analyzer and the sample surface was 45 degrees. The peak position of C1s was calibrated by adjusting the 285.0 eV.

**Surgical Procedure**

The experimental implants were placed in sixty 8-week-old male Sprague Dawley rats according to the method of Okamoto et al<sup>9)</sup>. The rats were placed under general anesthesia by inhalation of isoflurane (Forane®, Abbott Japan Co., Ltd., Tokyo, Japan). Hair was shaved from around the knee joints on both sides, and an incision of approximately 15 mm was made from the knee joint along the anterior border of the tibia, exposing the bone. An implant cavity was created 10 mm below the knee joint, and the experimental implant was placed in the tibia. Implant placement was carried out very cautiously to ensure no damage to the titanium coating. The wound was sutured after placement of the implants, thus completing the surgical procedure. An antibiotic (VICCILIN®; Meiji Seika Pharma Co., Ltd., Tokyo, Japan) was administered by intraperitoneal injection to prevent postoperative infection. This study was approved by the Animal Experimentation Committee of Fukuoka Dental College (approval number 13002). Five rats on each group SA and AE were sacrificed at 3, 5, 10, 14, 21 and 28 days after implant placement. Specimens were collected for

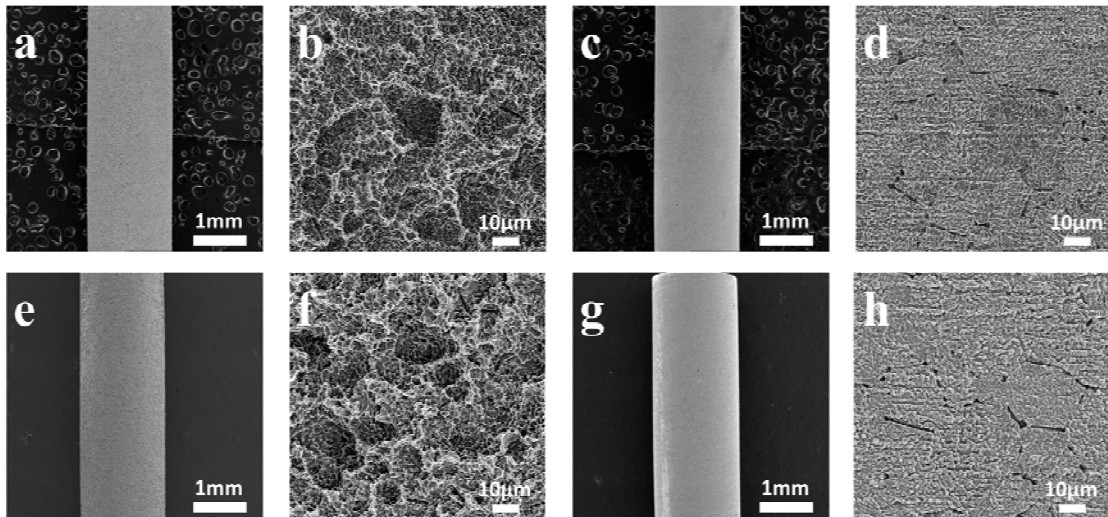


Figure 3. SEM image of the experimental implant. Titanium rod: Sandblasted and acid-etched: (a, b); Titanium rod: Acid-etched: (c, d); Experimental implant: Sandblasted and acid-etched: (e, f); Experimental implant: Acid-etched: (g, h).

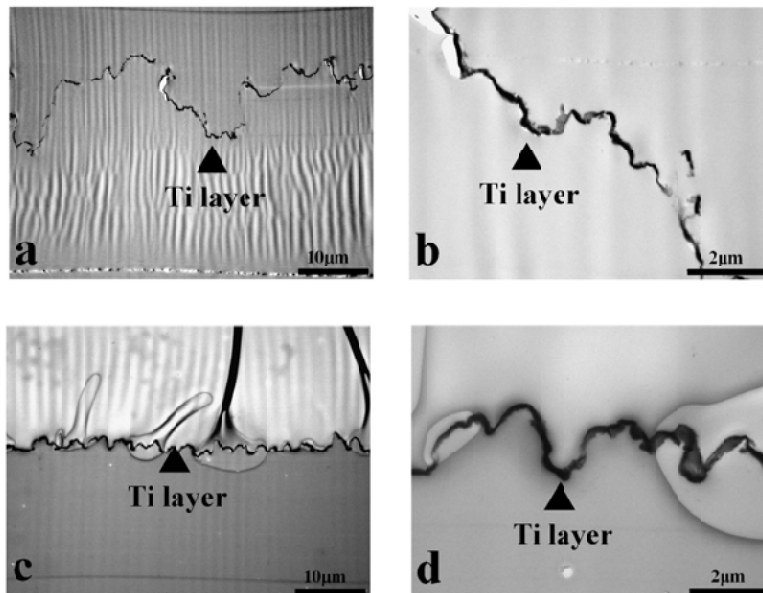


Figure 4. TEM image of the experimental implant after titanium coating. The experimental implant was embedded in epoxy resin, and ultrathin sections were prepared to examine the titanium layer. The titanium layer covers the irregularities of the plastic implant. a: Sandblasted and acid-etched; b: Sandblasted and acid-etched; c: Acid-etched; d: Acid-etched. Bar=10µm (a, c). Bar=2µm (b, d).

examinations of experimental implants and peri-implant bone.

#### Micro Computed Topography Examination

Experimental animals were sacrificed at 3, 5, 10, 14, 21 and 28 days, and the experimental implants and the peri-implant bone were harvested. The samples were wrapped in Parafilm® to prevent them from drying out and stored. Imaging of the samples was carried out using micro-computed tomography (micro-CT) (SkyScan 1176; Bruker micro CT, Kontich, Belgium). Imaging conditions were: tube voltage, 50 kV; tube current, 500 µA; and slice width, 8.81 µm. The samples were imaged simultaneously with a standard bone mineral reference phantom. Approximately 600 slices were required for imaging the experimental implant and peri-implant bone. The CT data were transferred to a

workstation, and a 3D reconstruction was created using three-dimensional trabecular structure measurement software (TRI/3D-BON, Ratoc System Engineering Co., Ltd., Tokyo, Japan). The bone marrow regions were extracted from the reconstructed 3D image, and bone volume/tissue volume (BV/TV, %) and bone mineral density (BMD, mg/cm<sup>3</sup>) in the bone marrow region surrounding the implant were measured. Measurements were taken at six sites for each implant, each site comprising 10 concentric half-tubes 300 µm high and 0-88.1 µm thick arranged 0-88.1 µm outward from the implant surface toward the existing bone and bone marrow (Fig. 2). The measurement values thus obtained were compared by distance from the implant surface and number of days after implant placement.

Table 2. Comparison of surface roughness. Surface roughness measurements were made at three sites per sample, and three experimental implants of each type were measured.

	Sa ( $\mu\text{m}$ )	Sdr (%)
Sandblasted and acid-etched (SA)	2.68±0.536	313.22±18.858
Acid-etched (AE)	0.47±0.069	119.65±23.601

Table 3. Evaluation by X-ray spectroscopic analysis (XPS). The main elements detected were Ti, O, and C.

	Ti	O	C	Na	Si	Cl
Sandbrasted and acid-etched (SA)	13.4	47.2	37.2	-	2.0	0.2
Acid-etched (AE)	13.5	48.7	35.9	0.3	1.4	0.2 (atomic%)

### Preparation of Samples for Light Microscopy

Samples were harvested at 3, 10, 14, 21 and 28 days after implant placement. The experimental animals were placed under general anesthesia with ether (diethyl ether; Wako Pure Chemical Industries, Ltd., Osaka, Japan) (0.1 mg/100 g), and then pentobarbital sodium (Somunopentyl®; Kyoritsu Seiyaku Corp., Tokyo, Japan) was administered by intraperitoneal injection. Perfusion fixation was carried out through the aorta using half-strength Karnovsky fixative. The implant and peri-implant bone were harvested and immersed in fixative for 24 h. The samples were trimmed and then decalcified with 10 % ethylenediamine-tetraacetic acid for 4 weeks. The samples were post-fixed in 2 % osmium tetroxide solution and block stained in 0.25 % uranyl acetate. The samples were dehydrated with ethanol, which was substituted with propylene oxide, and embedded in epoxy resin (Epon 812, Taab) according to the usual protocol. Then, 1.0- $\mu\text{m}$ -thick sections were cut with a microtome, stained with toluidine blue, and examined under an optical microscope. Samples that were used for micro-CT measurement were also examined under an optical microscope after micro-CT imaging.

### Statistical Analysis

Statistical analysis was performed using the SPSS version 19 software (SPSS Inc., Chicago, IL, USA). Analyses were run in three determinations. Two-way repeated-measures analysis of variance (ANOVA) followed by Bonferroni's post-hoc tests or Student's t-test was performed to assess statistical difference. Data were considered significant at  $P < 0.05$ .

### Result

The surface characteristics of the samples were evaluated by SEM observation, surface roughness measurement, TEM observation, and surface analysis.

### Evaluation by SEM

At 20 $\times$  magnification, SA gave the impression of a rougher surface than AE (Fig. 3e, g). At 1,000 $\times$  magnification, small

irregularities were observed on the larger irregularities in SA (Fig. 3f). Small irregularities were observed in AE (Fig. 3h). No sites were found where the tips of the rough surface irregularities were rounded or the irregularities were not clear in either SA or AE (Fig. 3f, h). The surface of SA was not only rougher than that of AE, but it also presented distinctive surface characteristics (Fig. 3a-h).

Comparison of the titanium rod and the experimental implant confirmed that the implant faithfully reproduced the surface characteristics of the titanium rod (Fig. 3a-h).

### Evaluation of surface roughness

The Sa (the arithmetic average of the 3D height of the roughness) of the SA and AE experimental implants was 2.68±0.536  $\mu\text{m}$  and 0.47±0.069  $\mu\text{m}$ , respectively. The Sdr (the developed surface area ratio) of the SA and AE experimental implants was 313.22±18.858  $\mu\text{m}$  and 119.65±23.601  $\mu\text{m}$ , respectively (Table 2). Both Sa and Sdr were significantly higher in SA than AE.

### Evaluation by TEM

The titanium was coated in an almost completely even layer that followed the surface shape of the plastic rods that were made into the experimental implants. The titanium coating was a thin layer, approximately 100-120 nm thick (Fig. 4).

### Evaluation of surface characteristics

The surface composition of the titanium-coated experimental implants is shown in Table 3. The main elements in the surface composition of the two types of experimental implant were Ti, O, and C. The composition of SA was: Ti, 13.4%; O, 47.2%; and C, 37.2%. The composition of AE was: Ti, 13.5%; O, 48.7%; and C, 37.2%.

### Observation by micro-CT

#### 《BV/TV》

In SA, BV/TV increased suddenly from day 14 onward and

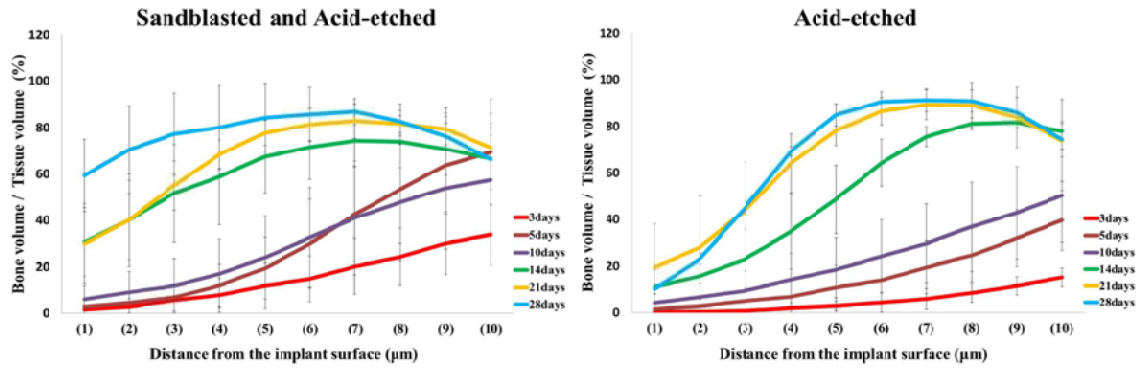


Figure 5. Bone Volume / Tissue Volume of peri-implant. In SA, BV/TV increased suddenly from day 14 onward and showed high values in the peri-implant region. In AE, BV/TV increased from day 21 and day 28. Distance from the implant surface: (1) 8.81 $\mu$ m-(10) 88.1 $\mu$ m.

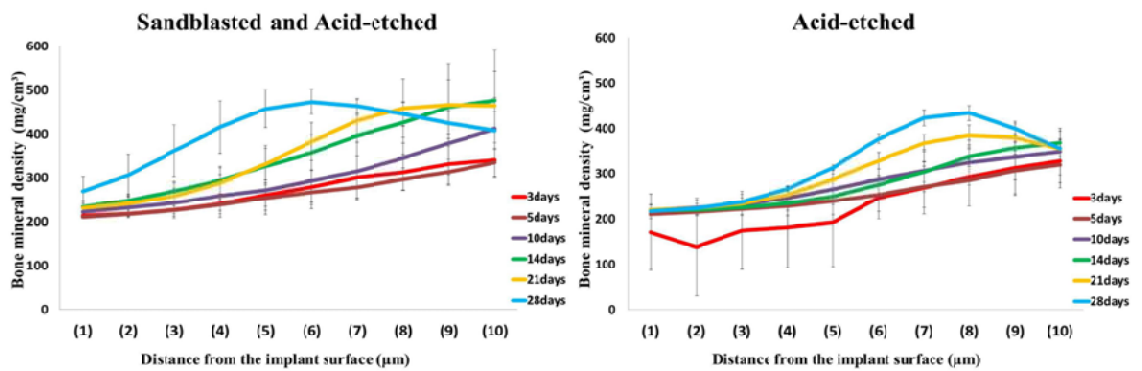


Figure 6. Bone Mineral Density of peri-implant. In the region up to approximately 50  $\mu$ m from the surface of the implant, BMD was significantly higher in SA than AE at day 28 ( $P < 0.05$ ). Distance from the implant surface: (1) 8.81 $\mu$ m-(10) 88.1 $\mu$ m.

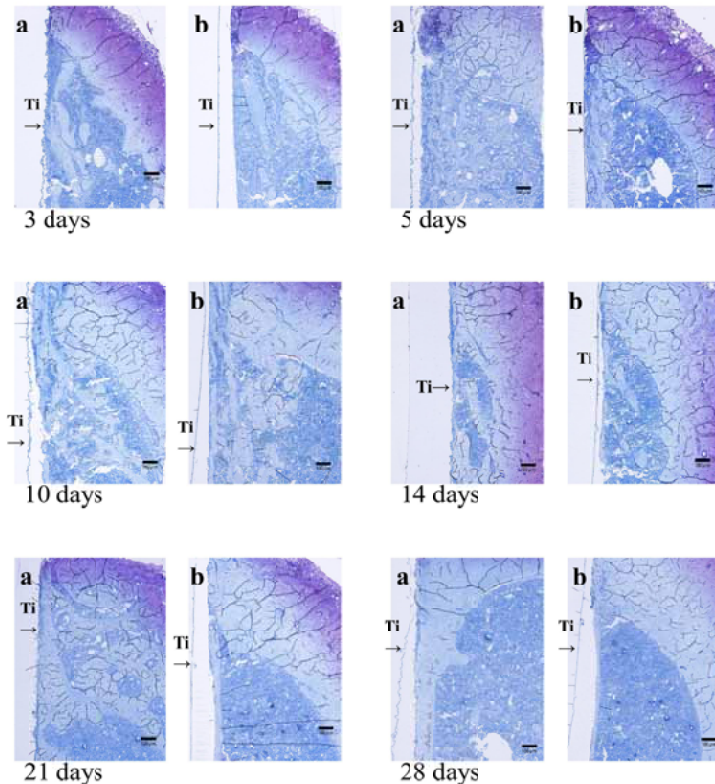


Figure 7. Light microscopy images 3 to 28 days after implant placement. a: Sandblasted and acid-etched (SA); b: Acid-etched(AE). Bar = 100 $\mu$ m

In some samples, the titanium-bone interface has become detached or the bone tissues have come apart during the preparation of sections for optical microscopy. This is probably due to the dehydration of the sample with ethanol prior to embedding. There were no obvious differences between SA and AE in the formation of new bone trabeculae.

showed high values in the peri-implant region. Further away from the surface of the implant, BV/TV showed a tendency toward constant values regardless of the length of time after implant placement.

In AE, an increase in BV/TV was found in the region a small distance from the peri-implant region. BV/TV increased at day 21 and 28 (Fig. 5).

#### «BMD»

In SA, peri-implant BMD showed constant low values from day 3 to day 21 after implant placement, and a high value at day 28.

In AE, an increase in BMD was found in the region a small distance away from the peri-implant area (approximately 50  $\mu\text{m}$  from the implant surface). Constant low values were found in the area near the implant surface.

In the region up to approximately 50  $\mu\text{m}$  from the surface of the implant, BMD was significantly higher in SA than AE at day 28 (Fig. 6).

#### *Observation by an optical microscope*

Observation by an optical microscope revealed new bone trabeculae in the peri-implant area in both SA and AE. No new bone was seen on the surface of the implant at day 3 after implant placement. New bone had formed at day 5, and new bone and existing bone were mixed together. Osteoblast-like cells were observed in the surroundings of the new bone. At day 10, there was far more new bone formation, and osseointegration was observed with bone in direct contact with the implant surface. At day 14, the formation of new bone trabeculae along the surface of the implant was observed. New bone trabecula formation was predominant from day 5 to day 10. The new bone seen on the implant surface was mature and finely detailed at 21 and 28 days. In both SA and AE, the thickness of new bone trabeculae increased at day 21. In AE there was no addition of bone to the bone marrow side, and the bone tissue matured without change, while in SA, the bone grew thicker on the surface of the implant.

There were no obvious differences between SA and AE in the formation of new bone trabeculae (Fig. 7).

#### **Discussion**

Osseointegration is currently regarded as an essential condition for the success of implants<sup>10, 11</sup>). Achieving osseointegration in the shortest possible time helps reduce the treatment period, which leads to early recovery of the patient's lost mastication function. Various different types of surface processing have been carried out on implants with the aim of strengthening osseointegration and reducing the time taken for it to be achieved<sup>1-5</sup>).

Histologic evaluation and measurement of removal torque

have been carried out on implants with various different surface characteristics<sup>12</sup>). The results have shown that rapid, strong osseointegration can be achieved with implants having surface roughness in the order of  $Sa=2 \mu\text{m}^{1-3}$ ). However, since the implant body is metal, tissue samples cannot readily be prepared, and, therefore, the tissue reaction at the titanium-bone interface cannot be easily evaluated<sup>9, 13-15</sup>).

Watazu et al.<sup>6-8</sup>) created a thin layer of titanium on the surface of plastic implants using DC magnetron sputtering, enabling Okamatsu et al.<sup>9</sup>) to observe osseointegration by optical microscopy and TEM. Morinaga et al.<sup>16</sup>) were able to make chronological observations of mineralized tissue surrounding a similar experimental implant using micro-CT. However, the previous experimental implants had smooth surfaces<sup>9, 16-19</sup>), and the reaction of the peri-implant tissue is therefore expected to be different from that of the rough-surfaced implants that are currently commonplace in clinical work. The present study compared differences in peri-implant tissue reactions to implants with two different types of surface characteristics.

The present study used experimental implants with SA and AE surface characteristics. Micro-CT is a method of microstructure analysis because it allows analysis at high resolution without disruption of the sample, and it allows description of the trabecular structure and quantification of bone volume and bone density<sup>16-18, 20-25</sup>). However, artifacts occur if the titanium body of the implant is present in the sample, so that the interface and peri-implant tissue cannot be accurately evaluated<sup>25, 26</sup>). If the implant is removed before evaluation, however, it is then no longer possible to evaluate the undamaged bone. In the present study, plastic-bodied implants with rough surfaces were therefore created in order to allow evaluation by micro-CT.

Chehroudi et al.<sup>15, 27-29</sup>) reported taking an impression of a rough-surfaced titanium disk with silicon impression material and then making a copy with epoxy resin. In the present study, titanium implants were first subjected to surface processing in order to create implants with two types of rough surface. Impressions of these titanium implants were then taken to produce plastic rods with the two types of rough surface (SA and AE). The rods were then coated with titanium by DC magnetron sputtering. Okamatsu et al.<sup>9</sup>) reported achieving a constant 150–250 nm titanium coating with the DC magnetron sputtering technique. Furthermore, Morinaga et al.<sup>16</sup>) were able to produce implants suitable for micro-CT observation of mineralized microstructure by shortening the sputtering time to produce a relatively thin titanium coating. In the present study, it was possible to create a thin layer of titanium on a rough plastic surface by carrying out sputtering at low power. This allowed the deposition of a thin layer of titanium, about 100–120 nm thick, that conformed to the surface microstructure.

The experimental implant thus created was examined by SEM and TEM, and the surface roughness and surface composition were

measured. Wennerberg *et al.* reported that evaluation of surface roughness of oral implants should be made with 3D measurement of three places on each of at least three samples. The surface roughness of the present implants was measured according to Wennerberg *et al.*<sup>30)</sup>, and the results showed that the two types of experimental implant faithfully recreated the surface characteristics of typical rough-surfaced implants available on the clinical practice. Albrektsson and Wennerberg *et al.*<sup>1-3)</sup> reported that roughness at the micro-level is an important factor in the reaction of bone to the implant, and they recommended comparing surface roughness using the arithmetic average of the 3D height of the roughness (Sa). Sa values for the experimental implants in the present study were  $2.68 \pm 0.54 \mu\text{m}$  for SA and  $0.47 \pm 0.07 \mu\text{m}$  for AE, which are classified as “rough” and “minimally rough”, respectively. The experimental implants created according to the method outlined above reproduced the surface form of the original titan implants. In addition, the surface composition was analyzed using XPS. The main elements detected were Ti, O, and C. Si, Na, and Cl were also detected, but these elements are among those reported by Morra *et al.*<sup>31, 32)</sup> on the surface of oral implants used in clinical practice.

In the micro-CT evaluation, BV/TV and BMD of peri-implant mineralized tissue were measured. In the 3D reconstruction image created from micro-CT images, no metal artifacts were seen that could obstruct observation of the peri-implant region. Micro-CT is reported to be the most suitable method of observation for 3D structural analysis of trabeculae, but there are limits to the materials that will allow imaging. The plastic implants created in the present study were not affected by metal artifacts in the micro-CT imaging, so that it was possible to observe the peri-implant cancellous bone structure with clarity.

BMD measurement in AE showed that, in the bone marrow region, the mineralization progressed in the region a small distance away from the implant. This is the same as the finding reported by Morinaga *et al.*<sup>17)</sup>. Furthermore, the BMD value was higher in SA than in AE at day 28 after placement of the implant, when osseointegration was complete, and the BV/TV value was high at an earlier stage in SA than AE. Progress in mineralization in the region near the surface of the implant is likely to be beneficial in achieving osseointegration.

Albrektsson *et al.*<sup>1-3)</sup> reported strong bone tissue reaction and better clinical outcomes with implants of medium roughness ( $1.0\text{--}2.0 \mu\text{m}$ ) than with machine-processed implants. In addition, numerous researchers reported that implants with optimal surface characteristics have high removal torque earlier after implant placement than implant bodies with comparatively smooth surfaces<sup>33)</sup>. The results of the present study showed that, with implants with rough surfaces that are considered optimal, mineralization of peri-implant bone progresses close to the implant surface. This strongly supports the results of basic and clinical

research to date into implant surface characteristics.

In conclusion, in this study, newly developed experimental titanium-coated implants faithfully reproduced the surface characteristics of typical rough-surfaced implants. No metal artifacts were detected on CT examination, so that the experimental implants are suitable for examination of the intact titanium-bone interface.

The peri-implant bone tissue reaction was compared between experimental implants with two types of surface characteristics (SA and AE). The following results were obtained.

1. Histological examination of bone trabecula formation showed no great difference between SA and AE. New bone was formed from day 5 onward, and at day 10, bone tissues that had formed in different sites adhered to each other. At day 14, lamellar bone had formed along the surface of the implant. At days 21-28, the thickness of the lamellar bone covering the peri-implant region had increased.

2. With AE, the BMD of peri-implant trabecular bone showed that bone mineralization progressed not on the surface of the implant but at sites a small distance away. At day 28 after placement of the implant, when osseointegration was complete, the BMD value in the region near the implant surface was higher in SA than AE. Furthermore, the BV/TV value was high at an earlier stage in SA than AE. The results showed that the SA surface is more beneficial for achieving osseointegration than AE.

#### Acknowledgements

We want to thank Dr. Kazuhiko Okamura and Mr. Koichiro Morishita, Department of Morphological Biology, Fukuoka Dental College, for their valuable advice and support. This work was partly supported by Strategic study base formation support business (S1001059) from the Ministry of Education, Culture, Sports, Science and Technology of Japan.

#### References

1. Wennerberg A and Albrektsson T. On implant surfaces: a review of current knowledge and opinions. *Int J Oral Maxillofac Implants* 25: 63-74, 2010
2. Albrektsson T and Wennerberg A. Oral implant surfaces: Part 1-review focusing on topographic and chemical properties of different surfaces and in vivo responses to them. *Int J Prosthodont* 17: 536-543, 2004
3. Albrektsson T and Wennerberg A. Oral implant surfaces: Part 2-review focusing on clinical knowledge of different surfaces. *Int J Prosthodont* 17: 544-564, 2004
4. Shalabi MM, Gortemaker A, Van't Hof MA, Jansen JA and Creugers NH. Implant surface roughness and bone healing: a systematic review. *J Dent Res* 85: 496-500, 2006
5. Dohan Ehrenfest DM, Vazquez L, Park YJ, Sammartino G and Bernard JP. Identification card and codification of the

- chemical and morphological characteristics of 14 dental implant surfaces. *J Oral Implantol* 37: 525-542, 2011
6. Watazu A, Teraoka K, Kido H, Okamatsu K, Nagashima Y, Morita M, Matsuura M and Saito N. Formation and properties of transparent titanium thin films by DC magnetron sputtering for observing interactions between titanium and cells. *Trans Mater Res Soc Jpn* 31: 677-680, 2006
  7. Watazu A, Kido H, Beppu K, Teraoka K, Morinaga K, Kakura K, Sonoda K and Saito N. Observation of interaction between living bone and micro implant with titanium thin film. *J Aust Ceram Soc* 47: 56-60, 2011
  8. Watazu A, Sakai T, Teraoka K, Sonoda T, Morinaga K and Kido H. Formation of calcium phosphate / titanium oxide/ titanium/ plastic composite implant. *Key Eng Mater* 529-530: 531-536, 2013
  9. Okamatsu K, Kido H, Sato A, Watazu A and Matsuura M. Ultrastructure of the interface between titanium and surrounding tissue in rat tibiae - A comparison Study on titanium-coated and uncoated plastic Implants. *Clin Implant Dent Relat Res* 9: 100-111, 2007
  10. Albrektsson T, Johansson C and Sennerby L. Biological aspects of implant dentistry: osseointegration. *Periodontol* 2000 4: 58-73, 1994
  11. Albrektsson T, Brånemark PI, Hansson HA and Lindström J. Osseointegrated titanium implants. Requirements for ensuring a long-lasting, direct bone-to-implant anchorage in man. *Acta Orthop Scand* 52: 155-170, 1981
  12. Buser D, Schenk RK, Steinemann S, Fiorellini JP, Fox CH and Stich H. Influence of surface characteristics on bone integration of titanium implants. A histomorphometric study in miniature pigs. *J Biomed Mater Res* 25: 889-902, 1991
  13. Ayukawa Y, Takeshita F, Inoue T, Yoshinari M, Ohtsuka Y, Murai K, Shimono M and Suetsugu T. An ultrastructural study of the bone-titanium interface using pure titanium-coated plastic and pure titanium rod implants. *Acta Histochem Cytochem* 29: 243-254, 1996.
  14. Ayukawa Y, Takeshita F, Yoshinari M, Inoue T, Ohtsuka Y, Shimono M, Suetsugu T and Tanaka T. An immunocytochemical study for lysosomal cathepsins B and D related to the intracellular degradation of titanium at the bonetitaniuminterface. *J Periodontol* 69: 62-68, 1998
  15. Listgarten MA, Buser D, Steinemann SG, Donath K, Lang NP and Weber HP. Light and transmission electron microscopy of the intact interfaces between non-submerged titanium-coated epoxy resin implants and bone or gingiva. *J Dent Res* 71: 364-371, 1992
  16. Morinaga K, Kido H, Sato A, Watazu A and Matsuura M. Chronological changes in the ultrastructure of titanium-bone interfaces: analysis by light microscopy, transmission electron microscopy, and micro-computed tomography. *Clin Implant Dent Relat Res* 11: 59-68, 2009
  17. Morinaga K, Kido H, Sato A, Kae K, Watazu A, Teraoka K, Beppu K and Matsuura M. Observation of microstructures between the bone-titanium implant interfaces by means of micro-CT. *Jpn J Maxillofac Implants* 6: 213-218, 2007
  18. Beppu K, Kido H, Watazu A, Teraoka K and Matsuura M. Peri-implant bone density in senile osteoporosis-changes from implant placement to osseointegration. *Clin Implant Dent Relat Res* 15: 217-226, 2013
  19. Sakai T, Okamura K, Watazu A, Teraoka K and Kido H. The effect of implant surfaces sputter-coated with hydroxyapatite target. *J Hard Tissue Biol* 22: 67-78, 2013
  20. Stauber M and Müller R. Micro-computed tomography: a method for the non-destructive evaluation of the three-dimensional structure of biological specimens. *Methods Mol Biol* 455: 273-292, 2008
  21. Nakada H, Suwa T, Numata Y, Okazaki Y, Machida T, Gunji A, Sakae T, Hayakawa T, Kato T, Wada M and Kobayashi K. Micro-CT study of newly formed bone around Ti implants with different surface treatment - Structure of trabecula bone and measurement of bone mineral density. *J Jpn Assoc Regenerative Dent* 3: 24-40, 2005
  22. Takahashi Y, Arimoto M, Shinoda K, Yamamoto I and Morimoto K. Observation of the bone-implant interface using microfocus x-ray CT system. *J Jpn Soc Dent Mater Devices* 22: 353, 2003
  23. Shalabi MM, Wolke JG, Cuijpers VM and Jansen JA. Evaluation of bone response to titanium-coated polymethyl methacrylate resin (PMMA) implants by X-ray tomography. *J Mater Sci Mater Med* 18: 2033-2039, 2007
  24. Azuma Y, Harada Y, Takagi H, Kamimura T, Ohta T and Yamada N. Micro-focused x-ray computed tomography for three-dimensional analysis of trabecular bone. *J Jpn Soc Bone Morphom* 10: 53-61, 2000
  25. Butz F, Ogawa T, Chang TL and Nishimura I. Three-dimensional bone-implant integration profiling using micro-computed tomography. *Int J Oral Maxillofac Implants* 21: 687-695, 2006
  26. Walker SS, Kontogiorgos ED, Dechow PC, Kerns DG, Nelson CJ and Opperman LA. Comparison of the effects of phosphate-coated and sandblasted acid-etched titanium implants on osseointegration: a microcomputed tomographic examination in the canine model. *Int J Oral Maxillofac Implants* 27: 1069-1080, 2012
  27. Chehroudi B, Gould TR and Brunette DM. The role of connective tissue in inhibiting epithelial downgrowth on titanium-coated percutaneous implants. *J Biomed Mater Res* 26: 493-515, 1992
  28. Wieland M, Chehroudi B, Textor M and Brunette DM. Use



Kazuko Yamamoto *et al.*: The Effects of Implant Surface Characteristics on Surrounding Bone

- of Ti-coated replicas to investigate the effects on fibroblast shape of surfaces with varying roughness and constant chemical composition. *J Biomed Mater Res* 60: 434-444, 2002
29. Kim H, Murakami H, Chehroudi B, Textor M and Brunette DM. Effects of surface topography on the connective tissue attachment to subcutaneous implants. *Int J Oral Maxillofac Implants* 21: 354-365, 2006
  30. Wennerberg A and Albrektsson T. Suggested guidelines for the topographic evaluation of implant surfaces. *Int J Oral Maxillofac Implants* 15: 331-344, 2000
  31. Morra M, Cassinelli C, Bruzzone G, Carpi A, Di Santi G, Giardino R and Fini M. Surface chemistry effects of topographic modification of titanium dental implant surfaces: 1. Surface analysis. *Int J Oral Maxillofac Implants* 18: 40-45, 2003
  32. Cassinelli C, Morra M, Bruzzone G, Carpi A, Di Santi G, Giardino R and Fini M. Surface chemistry effects of topographic modification of titanium dental implant surfaces: 2. *In vitro* experiments. *Int J Oral Maxillofac Implants* 18: 46-52, 2003
  33. Gotfredsen K, Berglundh T and Lindhe J. Anchorage of titanium implants with different surface characteristics: an experimental study in rabbits. *Clin Implant Dent Relat Res* 2: 120-128, 2000

